Neutron-diffraction study of the magnetic structures in RD_2 (R = Tb, Dy, Ho, and Er)

H. Shaked

Nuclear Research Center, Negev, POB 9001 and Ben-Gurion University, Negev, POB 653, Beer-Sheva, Israel

D. G. Westlake, J. Faber, Jr., and M. H. Mueller

Argonne National Laboratory, Argonne, Illinois 60439

The magnetic structures in cubic RD_2 (R = Tb, Dy, Ho, and Er) have been studied with neutron diffraction. The dideuterides of Tb, Dy, and Ho have modulated magnetic structures with a periods of $4a_0/\sqrt{11}$ along [113]. This modulation is commensurate with the crystal lattice and leads to a nonprimitive cubic magnetic lattice with a translation of $4a_0$. The ionic magnetic moments are of a single magnitude, independent of position. The magnetic structure of ErD_2 contains both a commensurate component that belongs to a cubic magnetic lattice with lattice parameter $4a_0$ and an additional incommensurate component. An intermediate magnetic structure of the type found in ErD_2 appears in the Tb, Dy, and Ho compounds above T_N, but disappears below T_N, giving way to the apparently more stable, commensurate structure mentioned above.

I. INTRODUCTION

The rare-earth metals form hydrides that have been the subject of many studies.[1-3] The dihydrides, RH_2 (R represents rare earth), crystallize in the cubic fluorite structure[1] (Fig. 1) and have a finite range of stable compositions, both hypo- and hyperstoichiometric. In the hypostoichiometric dihyrides, when [H]/[R] approaches 2.0, a small fraction of the H atoms begins to fill the octahedral sites[4] located at the body center of the cube and at the midpoints of the cube edges (Fig. 1). Some of the paramagnetic RH_2 compounds undergo a transition to antiferromagnetism at low temperatures.[1,2,5-10] The crystalline electric field (CEF) plays an important role in the magnetism of these compounds.[5-8,11,12] For the R site with all neighboring octahedral sites vacant, the CEF is

FIG. 1. Crystallographic unit cell for the dihydride of a rare-earth metal.

totally different than it is if one octahedral site is occupied by hydrogen. For this reason, the magnetic properties of these dihydrides, may change drastically as the [H]/[R] value varies over the range of stable compositions.[7] In the study of magnetic structures of hydrides with neutron scattering, D is used rather than H. This substitution was not expected to affect the conclusions of the study, because measurements[5-9] of specific heat, magnetic susceptibility, and the Mössbauer effect indicate that there is no isotope effect on the magnetic properties. The magnetic structure of only one dihydride, TbD_2, is reported[10] in the literature. It is a collinear structure with the edge of the cubic unit cell measuring $4a_0$. That investigation was the first part of a neutron-diffraction study of a group of RD_2 compounds with R = Tb, Dy, Ho, and Er. This paper reports the results for all four of these dideuterides. A complete magnetic structure determination was achieved only for R = Tb and Ho. Important information was deduced, however, regarding the magnetic structures with R = Dy and Er. A propagation vector which is commensurate with the reciprocal chemical lattice has been used in the search for the magnetic structure. This gave a simpler and more elegant description of the magnetic structure than the one used in the earlier paper.[10]

II. EXPERIMENT

Samples of Tb, Ho, and Er were obtained from Alfa Products, Danvers, Massachusetts, and the Dy was obtained from the United Mineral and Chemical Corporation, New York, NY. The dideuterides were prepared by heating the metals to 1075 K in a vacuum better than 3×10^{-4} Pa and reacting them with a measured quantity of D_2 gas as they cooled to 575 K over a period of 6 h. Purified D_2 was obtained by thermal decomposition of UD_3. The resulting dideuterides were pulverized, sieved, and encapsulated in vanadium sample holders.

Neutron spectra were taken with short- (~ 1.0 Å) and long (~ 2.4 Å) wavelength neutrons at the CP-5 (Ar-

gonne National Laboratory) and IRR-2 (Nuclear Research Center, Negev) reactors. Some of these spectra are shown in Fig. 2. All of the indices correspond to a cubic lattice with translation $4a_0$, where a_0 is the cubic chemical lattice translation (Fig. 1). Hence, the nuclear reflections {111} and {200} of the fcc chemical lattice appear here as {444} and {800}. The other indices are of the all-odd type. Of these, a certain type is missing (line extinction), namely, $(111) \pm T$, where the T's are reciprocal chemical lattice translations such as (444), ($\bar{4}$44),...,(800), (080), etc.
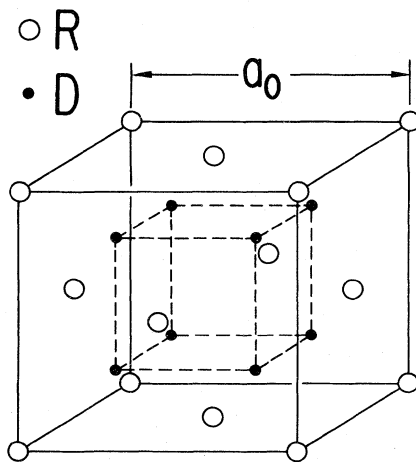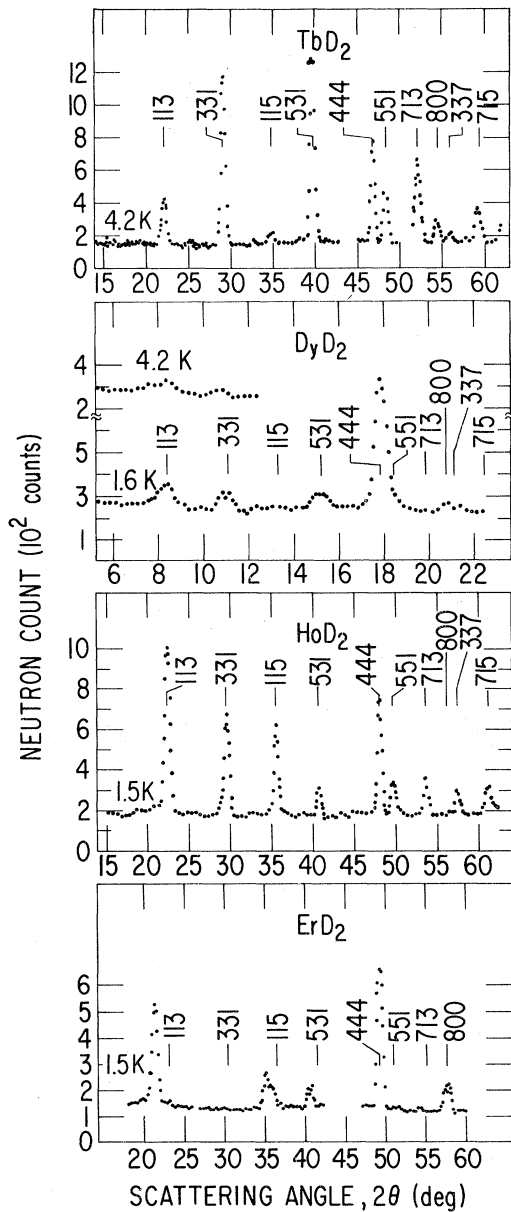
FIG. 2. Neutron-diffraction spectra of RD_2 (R =Tb, Dy, Ho, and Er) at low temperatures. The spectra are indexed according to a cubic lattice with a translation of $4a_0$. The observed magnetic reflections of ErD$_2$ do not fall in the all-odd positions of the reciprocal lattice.

A. TbD$_2$

During cooling, magnetic reflections appear at 17.2 K.[10] They index as all-odd reflections with the aforementioned line extinction. Relatively weak reflections of an intermediate magnetic structure appear above T_N but disappear below T_N.[10] One of these reflections can be indexed as {541} and is shown in Fig. 4 of the previous work.[10] The integrated intensities of the reflections in the 4.2-K spectrum are listed in Table I.

B. DyD$_2$

Two samples of DyD$_2$ were prepared. Because of the high neutron absorption in Dy, it was necessary to use a flat, 3-mm-thick specimen holder and short-wavelength (0.94-Å) neutrons. The first sample, with [D]/[Dy]~2.06, was studied by neutron diffraction at temperatures down to 1.4 K, but it showed no magnetic reflections. Measurement[13] of the Mössbauer effect in this sample revealed no hyperfine structure at temperatures down to 1.6 K. The second sample, however, with [D]/[Dy]~1.96 did exhibit full hyperfine splitting in the Mössbauer spectrum at 1.6 K (Ref. 13) [as did the dihydride of Dy (Ref. 8)]. The neutron spectrum of this deuteride at 1.6 K showed magnetic reflections (Fig. 2) that appeared at the same positions as the reflections from TbD$_2$. Magnetic reflections are also apparent at 4.2 K (Fig. 2). An attempt to determine the transition temperature was unsuccessful because of the low intensity. A weak reflection from the intermediate magnetic structure is observed (Fig. 2) near {113} at 4.2 K.

C. HoD$_2$

The magnetic reflections in the 1.5-K spectrum (Fig. 2) appear at exactly the same positions as those in the Tb and Dy spectra. The emergence and temperature dependence of the {113} reflection is shown in Fig. 3. The reflection appears at about 9 K, accompanied by a reflection from the intermediate magnetic structure (on the low-angle side). It is only when the line from the intermediate structure disappears below 4 K that the intensity of the {113} reflection increases in a "first-order" fashion to nearly its saturated value. The reflection from the intermediate structure (Fig. 4) has $s^2 = 9.60$ (where $s^2 = h^2 + k^2 + l^2$) and, hence, it is incommensurate with the $4a_0$ cubic lattice. The integrated intensities of the reflections in the spectrum for 1.5 K are listed in Table I. There is a discrepancy between the calculated and the observed nuclear intensities. The observed intensity ratio for {444}:{800}:{880} is approximately 20:1:60. It fits calculated intensities where the scattering amplitude of D is reduced by 16%. This ratio cannot be obtained by setting some D atoms in octahedral sites. The source of this discrepancy is not entirely clear to us. It could be only in part due to D deficiency (16% deficiency in D is outside the stoichiometry range[3]). The error in the nuclear intensities propagates into the calculation of the magnitude of the magnetic moment (MMM). The resulting error in MMM is smaller than the discrepancy in the square root of the intensity ratio, which is smaller than 8%.

TABLE I. Observed integrated intensities and the calculation of the form factor (see the Appendix).

s^2	$h\ k\ l$	θ^a	L^b	$\dfrac{\sin\theta^c}{\lambda}$	JF^{2d} TbD$_2$	HoD$_2$	TbD$_2$ $I^{obs}(\sigma)$	$f^{obs}(\sigma)^e$	HoD$_2$ $I^{obs}(\sigma)$	$f^{obs}(\sigma)^f$
11	1 1 3	11.11	13.723	0.0797	1.454	7.075	2420(90)	0.961(19)	6870(120)	0.980(9)
19	3 3 1	14.66	8.069	0.1048	7.579	7.642	7000(110)	0.934(7)	4120(100)	0.953(12)
27	1 1 $\bar{5}$	17.56	5.761	0.1249	0.5926	7.474	430(70)	0.979(90)	2830(90)	0.944(15)
35	$\begin{cases}\bar{5}\ 3\ 1\\ 3\ \bar{5}\ 1\end{cases}$	20.09	4.512	0.1422	15.543	3.058	7240(110)	0.887(7)	900(70)	0.921(38)
51	5 5 $\bar{1}$	24.50	3.195	0.1717	7.843	7.919	2480(80)	0.868(14)	1480(80)	0.890(25)
59	$\begin{cases}\bar{7}\ 1\ 3\\ 1\ \bar{7}\ 3\end{cases}$	26.49	2.808	0.1846	13.559	8.300	3800(100)	0.850(11)	1280(80)	0.863(28)
67	3 3 $\bar{7}$	28.38	2.515	0.1968	2.142	7.718	460(70)	0.805(61)	980(70)	0.845(30)
75	$\begin{cases}7\ \bar{1}\ 5\\ \bar{1}\ 7\ 5\end{cases}$	30.19	2.288	0.2082	9.820	8.974	1840(80)	0.790(21)	1020(100)	0.821(40)
48	4 4 4	23.72	3.374		36.966	46.240	4070(90)		3920(100)	
64	8 0 0	27.68	2.617		15.81	11.244	1030(50)		200(100)	

$^a\ \theta = \arcsin(s/17.22)$.

$^b\ L = (\sin\theta\,\sin2\theta)^{-1}$.

$^c\ \sin\theta/\lambda = s/41.6$.

$^d\ jF^2 = \sum_G P^2$ for the magnetic reflections.

$^e\ f^{obs} = 0.087\,273(I^{obs}/LjF^2)^{1/2}$.

$^f\ f^{obs} = 0.115\,315(I^{obs}/LjF^2)^{1/2}$.
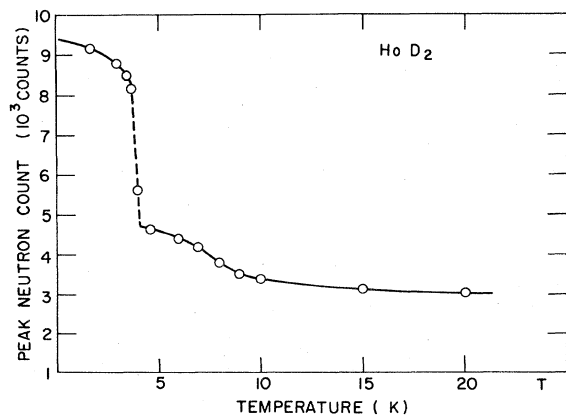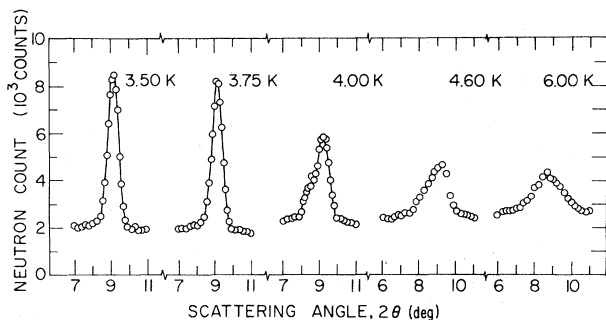
FIG. 3. Emergence of the {113} line. Peak scans at several temperatures (above). Peak-intensity—temperature curve (below). Wavelength of neutrons ~0.99 Å.

D. ErD$_2$

The spectrum of ErD$_2$ at 1.5 K (Fig. 2), taken with a flat, 3-mm-thick sample holder, shows four magnetic reflections. The positions of these reflections are different from the positions for the three preceding compounds. The s^2 values for the ErD$_2$ reflections are 9.6, 25, 26, and 33. The following indices correspond to the last three reflections: {500,430}, {510,431}, and {522,441}. The temperature dependence of the intensity of the first reflection (Fig. 5) yields $T_N = 2.15 \pm 0.05$ K, in excellent agreement with $T_N = 2.13 \pm 0.03$ K obtained by measurement[5] of the specific heat.
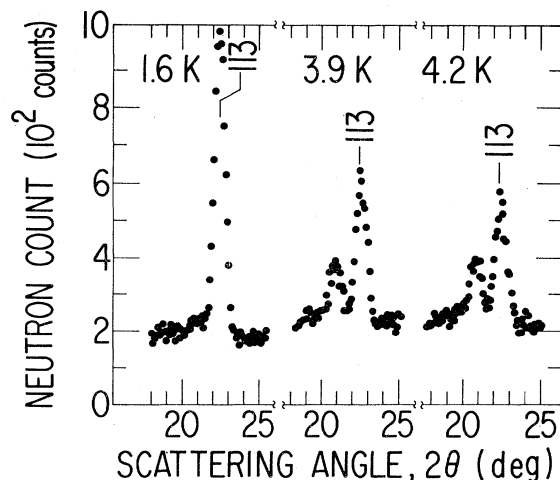
FIG. 4. Peak scans of the {113} reflection of HoD$_2$ at three different temperatures. Wavelength of neutrons ~2.4Å.
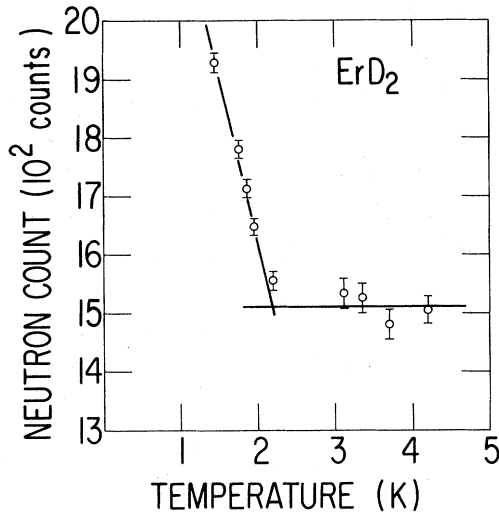
FIG. 5. Peak-intensity—temperature curve for the reflection near the {113} position in the ErD_2 spectrum. Wavelength of neutrons ~2.4 Å.

FIG. 6. Proposed spin structures for TbD_2 and HoD_2.

III. MAGNETIC STRUCTURE

All of the magnetic reflections for the dihydrides of Tb, Dy, and Ho can be considered as satellites of the reflections of the fcc chemical lattice formed by the propagation vector $2\pi[113]$ (Table II). Consequently, the magnetic structure is modulated along [113] with a period of $4a_0/\sqrt{11}$ (Fig. 6). It is convenient to describe the corresponding spin structure with the Cartesian coordinates $(\vec{k}_1, \vec{k}_2, \vec{k}_3) = (2\pi[\bar{3}\bar{3}2], 2\pi[1\bar{1}0], 2\pi[113])$.

The sharp, hyperfine lines in the Mössbauer spectra[6-8] suggest that the structure is collinear and has ionic magnetic moments which are independent of position. The following spin function is consistent with these suggestions:

$$\vec{S}(\vec{r}) = \sqrt{2}\hat{S}\cos\left[\vec{k}_3 \cdot \vec{r} + \frac{\pi}{4}\right].$$

This spin function will produce reflections at, and only at, the positions observed for Tb, Dy, and Ho. The direction of the spin axis $\hat{S}$ determines the relative intensities of the reflections. In solving for $\hat{S}$, we looked for a best fit of $c(I^{obs}/L\sum P^2)^{1/2}$ for all G (c is a constant independent of G) to the published form factor f' (see Appendix).

A. TbD₂

The $(1\bar{1}0)$ plane (Fig. 6) was scanned by setting $\hat{s} = s_1\hat{k}_1 + s_3\hat{k}_3$ and $s_1^2 + s_3^2 = 1$. A best fit to the previously published[14] form factor was found (Fig. 7) at $(s_1, s_3) = [(2/11)^{1/2}, 3/\sqrt{11}]$. This result leads to $s_1\hat{k}_1 + s_3\hat{k}_3 = [001]$, as was reported earlier.[10] The spin structure is shown in Fig. 6. The resulting magnitude of the magnetic moment (see Appendix) is $(7.4\pm0.4)\mu_B$ compared with $(7.6\pm0.3)\mu_B$ reported previously.[10]

TABLE II. Satellites of the first four fcc forms of reflections produced by the propagation vector $2\pi[113]$.

h k l	h k l⁺	h k l⁻
0 0 0	1 1 3	$\bar{1}$ $\bar{1}$ $\bar{3}$
4 4 4	5 5 7	3 3 1
$\bar{4}$ 4 4	$\bar{3}$ 5 7	$\bar{5}$ 3 1
4 $\bar{4}$ 4	5 $\bar{3}$ 7	3 $\bar{5}$ 1
4 4 $\bar{4}$	5 5 $\bar{1}$	3 3 $\bar{7}$
8 0 0	9 1 3	7 $\bar{1}$ $\bar{3}$
0 8 0	1 9 3	$\bar{1}$ 7 $\bar{3}$
0 0 8	1 1 11	$\bar{1}$ $\bar{1}$ 5
8 8 0	9 9 3	7 7 $\bar{3}$
8 0 8	9 1 11	7 $\bar{1}$ 5
0 8 8	1 9 11	$\bar{1}$ 7 5
8 $\bar{8}$ 0	9 $\bar{7}$ 3	7 $\bar{9}$ $\bar{3}$
8 0 $\bar{8}$	9 1 $\bar{5}$	7 $\bar{1}$ 11
0 8 $\bar{8}$	1 9 $\bar{5}$	$\bar{1}$ 7 11
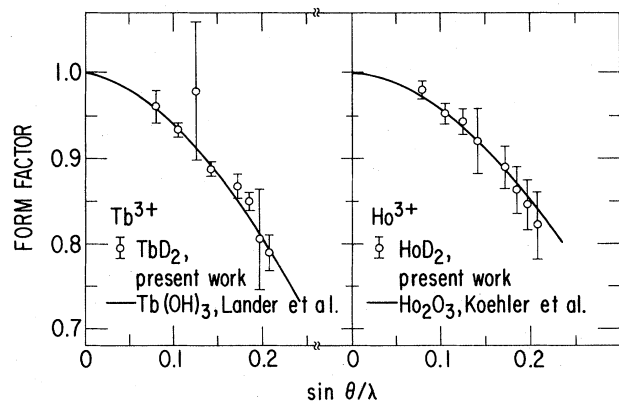
FIG. 7. Magnetic form factors of Tb^{3+} and Ho^{3+} as derived from I^{obs} for TbD_2 and HoD_2. The solid lines represent results previously obtained with $Tb(OH)_3$ (Ref. 14) and Ho_2O_3 (Ref. 15). The results of this work were scaled so that the first two reflections fit the solid lines.

B. DyD$_2$

The observed intensities are weak (Fig. 2), therefore no fit was attempted. The intensities of {331} and {531} are of similar magnitudes so that spin axis may be along [001]. One can estimate from the observed intensities that the magnitude of the magnetic moment is roughly $(3-4)\mu_B$. This is in agreement with Mössbauer results, where a moment of $3.8\mu_B$ was found.[8]

C. HoD$_2$

The $(3\bar{3}2)$ plane (Fig. 6) was scanned by setting $\hat{s}=s_2\hat{k}_2+s_3\hat{k}_3$ and $s_2^2+s_1^2=1$. A best fit to the previously published[15] form factor was found (Fig. 7) at (s_2,s_3) $=(0.94,0.34)$. This result leads to $s_2\hat{k}_2+s_3\hat{k}_3\sim$ $[8\bar{6}3]$, the closest symmetry axis being $[1\bar{1}0]$. The spin structure obtained is shown in Fig. 6. The resulting magnitude of the magnetic moment (Appendix) is $(6.4\pm0.4)\mu_B$.

D. ErD$_2$

The s^2 values for the four magnetic reflections that were observed (Fig. 2) are 9.60, 25, 26, and 33. Because the first reflection does not belong to the $4a_0$ lattice, the magnetic structure of ErD$_2$ consists of both commensurate and incommensurate components.

IV. SUMMARY AND DISCUSSION

Neutron diffraction was used to study the magnetic structures of RD$_2$ (R =Tb, Dy, Ho, and Er). The magnetic structures of the Tb, Dy, and Ho compounds are modulated with a period of $4a_0\sqrt{11}$ along [113]. These are commensurate structures where the magnitude of the moment is independent of position (Fig. 6). Collinearity was assumed in the search for the magnetic structure, in order to concur with Mössbauer-effect results.[6−8] This assumption is also justified a posteriori by the finding of collinear structures for which calculated intensities compare well with the observed intensities (Table I). The determination of the structure consists of a search for the direction of the spin axis. A spin axis was determined for the Tb and Ho compounds (Fig. 6), but the intensities for the Dy compound were too low to make a similar determination. The magnetic structure of ErD$_2$ was not determined, but it has an incommensurate component (hence a period different from $4a_0/\sqrt{11}$).

An intermediate magnetic structure was observed in the dihydrides of Tb,[10] Dy (Fig. 2), and Ho (Figs. 2, 3, and 4) above T_N, but it disappeared below T_N. The reflections from the intermediate structure are at the same positions as those of ErD$_2$ (Fig. 2); hence, the magnetic lattice of the intermediate structure in the Tb, Dy, and Ho compounds is identical to the magnetic lattice of ErD$_2$. Such a structure, therefore, is not unique to the Er^{3+} ion, but must be related to the symmetries of the crystal lattice.

The transition temperatures of the Tb, Dy, Ho, and Er deuterides are 17.2, 3.5, 4.5, and 2.15 K, respectively. This monotonic (except for Dy) decrease in T_N is in qualitative agreement with the de Gennes function

$(g-1)^2J(J+1)$, as is generally found in rare-earth compounds having indirect exchange [e.g., Ruderman-Kittel-Kasuya-Yosida (RKKY)] interactions.

A distribution of hyperfine fields, was observed[7,8] in DyH$_2$ at $3.3<T<6$ K and was attributed to short-range order (SRO). The reflection that we have observed from the intermediate magnetic structure in HoD$_2$ (Fig. 4) is sharp and characteristic of long-range order (LRO). It seems reasonable to expect that DyD$_2$ should also exhibit LRO, rather than SRO. We propose, therefore, that the distribution of hyperfines is caused by (i) the coexistence of the commensurate and the intermediate structures, and (ii) the incommmensurate component of the intermediate structure.

The paramagnetic-to-antiferromagnetic transitions in TbD$_2$ (Ref. 10) and HoD$_2$ (Fig. 3) are sharp and first-order-like. The magnetic moments of Tb^{3+} and Ho^{3+} are quenched by the CEF to $(7.4\pm0.4)\mu_B$ and $(6.4\pm0.4)\mu_B$, respectively, as compared to free-ion values of $9\mu_B$ and $10\mu_B$, respectively. A different contribution to this reduction may come from the loss of electrons to conduction. In Mössbauer-effect experiments[7] on HoD$_2$, a value of about 0.43 was observed for the ratio of the hyperfine field to the free-ion field. This is 33% lower than the value 0.64 found with neutrons in this work. The difference in these ratios, may be attributed to a difference in stoichiometries between the two samples.[7] An even more drastic dependence on stoichiometry was found in this work in the case of DyD$_2$ where a specimen with [D]/[Dy] >2 did not undergo any transition at all down to a temperature of 1.4 K; only the specimen with [D]/[Dy] <2 exhibited a transition.

In conclusion, further study is required for solution of the structure of ErD$_2$, which is related to the intermediate structures of TbD$_2$, DyD$_2$, and HoD$_2$. In addition, the relation between the ratio [D]/[R] and the existence of intermediate structures needs elucidation.

ACKNOWLEDGMENTS

APPENDIX: CALCULATED INTENSITIES

The integrated intensity of the magnetic reflection of neutrons from a powder sample at a given Bragg angle θ is

$$I=ALf^2p^2\sum_G P^2 , \qquad (A1)$$

where G, the length of reciprocal-lattice vector $\vec{G}$, is given by

$$G=4\pi\sin\theta/\lambda . \qquad (A2)$$

Here, λ is the neutron wavelength, A is a constant depending on geometry and instruments, L is the Lorentz factor and is equal to $(\sin\theta\sin2\theta)^{-1}$, f is the form factor at G, p is the magnetic scattering amplitude and is equal to

to $0.27n_B$, n_B is the magnetic moment in units of μ_B, P^2 is equal to $|\hat{G} \times \vec{F}_s|^2$, $\vec{F}_s$ is the spin structure factor and is equal to $\sum_r \vec{S}(r)\exp(i\vec{G}\cdot\vec{r})$, and $\vec{S}(\vec{r})$ is the spin function.

In search of the spin function, one uses (A1) to obtain the observed form factor as a function of G, namely

$$f^{obs} = c \left[I^{obs}/L \sum P^2 \right]^{1/2} . \tag{A3}$$

$\sum P^2$ and c are chosen to fit f, which is known from theory or from another experiment. After a spin structure is found, the scattering amplitude is calculated from

$$p^2 = \frac{j_N F_N^2}{j_M F_M^2} \frac{L_N}{L_M} \frac{1}{f_M^2} \frac{I_M^{obs}}{I_N^{obs}} , \tag{A4}$$

where the indices N and M stand for nuclear and magnetic, respectively, and $j_M F_M^2 = \sum_G P^2$. For the spin function

$$\vec{S}(\vec{r}) = \sqrt{2}\,\hat{S}\cos[\vec{k}_3 \cdot \vec{r} + (\pi/4)]$$

(Sec. III), the spin structure factor is $\vec{F}_s = 2\sqrt{2}\,\hat{s}$ per four spins and is independent of G. It follows that

$$P^2 = 8|\hat{G} \times \hat{S}|^2 = 8 \sum_{i,j=1,2,3} [\delta_{ij} - (\hat{G}\cdot\hat{k}_i)(\hat{G}\cdot\hat{k}_j)]s_i s_j ,$$
$$\tag{A5}$$

where s_i is the component of $\hat{s}$ along $\hat{k}_i$, and $\sum_{i=1}^{3} s_i^2 = 1$. A summary of the results obtained in applying these calculations to the I^{obs} of TbD_2 and HoD_2 is given in Table I where the following values were used:

$$j_M = 1, \quad j_N(444) = 4, \quad j_N(800) = 3 ,$$

$$b(Tb) = 0.76, \quad b(Ho) = 0.85 , \quad b(D) = 0.667 ,$$

$$(s_1, s_2, s_3) = \begin{cases} (\sqrt{2/11}, 0, 3/\sqrt{11}) & \text{for } TbD_2 \\ (0, 0.94, 0.34) & \text{for } HoD_2 . \end{cases}$$

[1]R. R. Arons, Landolt-Boernstein, Neue Ser. 12C, 372 (1982); W. G. Boss and K. H. Gayer, J. Nucl. Mater. 18, 1 (1960).

[2]W. E. Wallace, Ber. Bunsen-Gessel. 76, 832 (1972).

[3]G. G. Libowitz, Ber. Bunsen-Gessel. 76, 837 (1972).

[4]P. Vorderwisch and S. Hautecler, Phys. Status Solidi B 66, 595 (1974).

[5]Z. Bieganski and B. Stalinski, J. Less-Common Met. 49, 421 (1976); J. Opyrchal and Z. Bieganski, Solid State Commun. 20, 261 (1976).

[6]G. K. Shenoy, B. D. Dunlap, D. G. Westlake, and A. E. Dwight, Phys. Rev. B 14, 41 (1976).

[7]B. D. Dunlap, G. K. Shenoy, J. M. Friedt, and D. G. Westlake, J. Phys. (Paris) Colloq. 40, C5-211 (1979); J. M. Friedt, B. Suits, G. K. Shenoy, B. D. Dunlap, and D. G. Westlake, J.

Appl. Phys. 50, 2049 (1979).

[8]J. M. Friedt, G. K. Shenoy, B. D. Dunlap, D. G. Westlake, and A. T. Aldred, Phys. Rev. B 20, 251 (1979).

[9]R. L. Carlin and L. J. Krause, Phys. Rev. B 23, 6149 (1981).

[10]H. Shaked, J. Faber, Jr., M. H. Mueller, and D. G. Westlake, Phys. Rev. B 16, 340 (1977).

[11]H. Shaked and J. Faber, Jr., Phys. Rev. B 16, 4982 (1977).

[12]N. Shamir and H. Shaked, Phys. Rev. B 22, 6463 (1980).

[13]G. K. Shenoy (private communication).

[14]G. H. Lander, T. O. Brun, J. P. Desclaux, and A. J. Freeman, Phys. Rev. B 8, 3237 (1973).

[15]W. C. Koehler, E. O. Wollan, and M. K. Wilkinson, Phys. Rev. 110, 37 (1958).